Available online at www.sciencedirect.com

SciVerse ScienceDirect

Journal of Nutritional Biochemistry 22 (2011) 979–984

Journal of Nutritional Biochemistry

A mouse model for nonalcoholic steatohepatitis

Sinju Sundaresan[a,*], Parakat Vijayagopal[a], Nathaniel Mills[b], Vicky Imrhan[a], Chandan Prasad[a]

[a]Department of Nutrition and Food Sciences, Texas Woman's University, Denton, TX 76204, USA
[b]Department of Biology, Texas Woman's University, Denton, TX 76204, USA

Received 5 March 2010; received in revised form 31 May 2010; accepted 6 August 2010

Abstract

Background: Nonalcoholic steatohepatitis (NASH) is a hepatic manifestation of the growing metabolic syndrome epidemic that could progress to cirrhosis. Animal models adequately mimicking this condition in humans are scanty.
Aim: The objective of our study was to investigate whether high-fat diets (HFD) with adequate methionine and choline levels can induce pathophysiological features typical of human NASH in C57BL/6J mice.
Methods: Forty C57BL/6J mice, divided into control and high-fat (HF) groups, were fed low-fat diet and HFD, ad libitum respectively for 20 weeks. At the end of 20 weeks, animals were sacrificed and assays were performed for blood biomarkers typical of human NASH. Adipose tissue depots were collected and liver samples were processed for histological examination.
Results: High-fat feeding led to increased triglyceride accumulation in the liver (8.9 μmol/100 mg liver tissue vs. 2.6 μmol/100 mg for control) and induced histopathological features of human NASH including hepatic steatosis, ballooning inflammation and fibrosis. Expressions of proteins and chemokines predominant in NASH including collagens I, III and IV and platelet derived growth factor (PDGF) A and B were significantly higher in animals fed the HFD. Liver enzymes alanine transaminase, aspartate transaminase and alkaline phosphatase were significantly ($P<.05$) elevated in the HF group compared to controls. Mice on HFD also developed hyperglycemia, hyperinsulinemia, hypoadiponectinemia along with elevated tumor necrosis factor α, resistin, leptin, free fatty acids, transforming growth factor β and malondialdehyde levels that characterize NASH in humans.
Conclusion: Long-term HF feeding with adequate methionine and choline can induce many of the pathophysiological features typical of human NASH in C57BL/6J mice.
Published by Elsevier Inc.

Keywords: NASH; Insulin resistance; Fibrosis

1. Introduction

Nonalcoholic fatty liver disease (NAFLD) has become the most common chronic liver disease secondary to the growing epidemic of metabolic syndrome (MetS). A subset of the population with NAFLD progresses to nonalcoholic steatohepatitis (NASH). This population exhibits hepatic steatosis accompanied by inflammation and fibrosis [1]. NASH is considered to be the hepatic manifestation of MetS associated with obesity, non-insulin-dependent diabetes and hypertriglyceridemia [2].

Investigation of the molecular mechanisms of NASH and design of intervention studies is restricted by the availability of appropriate animal models that adequately mimic the spectrum of pathologic and pathophysiologic features associated with NASH. Among the various models and feeding regimens developed previously, intragastric overfeeding (for 9 weeks) resembles histopathology and pathophysiology of human NASH most closely [3]. However, stringent involvement of technical expertise and specialized equipment in this model has limited its widespread use. Alternatively, long-term studies using high-fat diets (HFDs) provided ad libitum were envisaged as potential prospects for inducing NASH just as closely to that seen in humans [4,5]. However, almost all models involving ad libitum feeding of HFD either mimic the histopathologic features (i.e., steatosis and fibrosing steatohepatitis) or the pathogenic correlates that include insulin resistance, oxidative stress and inflammation. Methionine and choline deficient (MCD) diets originally developed by Weltman et al [6] to induce steatohepatitis in rats and adapted to mice by Leclercq [7] produced hepatic inflammation and steatosis via increased CYP2E1 and CYP4A expression; however, the model did not exhibit insulin resistance, inflammation, or oxidative stress typical of NASH in humans. Collins et al [8] reported development of obesity and insulin resistance in the mouse model but could not develop noticeable steatohepatitis or fibrosis in C57BL/6J mice. The modified HFD (lower methionine and choline and higher fat) model developed recently by Cong et al [9] reproduced the typical histologic features and developed insulin resistance and dyslipidemia in the strain of mice; however, no evidence of state of inflammation or oxidative stress was reported. In the present study, a high-fat (HF) feeding regimen with adequate supply of methionine and choline was used to

* Corresponding author. Center for Human Nutrition, Department of Internal Medicine, Washington University School of Medicine, Campus Box 8031, St Louis, MO 63110, USA. Tel.: +1 314 362 8206; fax: +1 314 362 8230.
E-mail address: ssundare@dom.wustl.edu (S. Sundaresan).

0955-2863/$ - see front matter. Published by Elsevier Inc.
doi:10.1016/j.jnutbio.2010.08.011

induce NASH in C57BL/6J mice. A dilute solution of sucrose (0.2%) was used as drinking fluid in place of water to stimulate hyperphagia. Here, we present evidence that this mouse model on the feeding regimen used could serve as an excellent tool to examine the pathophysiology of human NASH based on observed changes in end points measured including body weight, adiposity, insulin resistance, oxidative stress and inflammation, liver histopathology and chemistry (free fatty acids, triglycerides, and selected liver enzymes).

2. Materials and methods

2.1. Animals and diets

C57BL/6J mice (n=40, age: 5 weeks) from Jackson Laboratories (Bar harbor, ME, USA) were acclimatized to the Texas Woman's University vivarium (temperature: 23–25°C, 12-h light/12-h dark, 50–60% humidity) for 1 week. All animal protocols were approved by the Institutional Animal Care and Use Committee. After acclimatization, animals were weighed and divided into two groups of 20 each. Experimental groups were fed HFD, while controls were maintained on low-fat diet for 20 weeks. To stimulate hyperphagia, experimental groups received 0.2% sucrose in water (w/v, changed daily) as the sole drinking fluid, while controls received tap water. Food and drinking fluids were available ad libitum. The HFD and low-fat diet were obtained in form of pellets from Harlan Teklad (Madison, WI, USA). The composition the HFD based on milk fat has been tailor-made to mimic actual Western diets leading to development of NASH (fatty acid composition: 12:0, 3%; C14:0, 10.3%; C16:0, 29.4%; C18:0, 12.6%; C18:1, 20.7%; C18:2, 2.3%; C18:3, 0.6%) and contained 21% w/w anhydrous milk fat vs. a control soybean oil diet containing 6% w/w fat (12% kcal from fat). Levels of methionine and choline in the HFD and low-fat diets were adequate (DL-methionine, 3 g/kg; choline bicitrate, 2.2 g/kg). The HFD was also high in sucrose (34% w/w), compared to 20% (w/w) in the low-fat diet. All other components including casein, corn starch, cholesterol, cellulose, vitamin and mineral mix were comparable in both diets.

2.2. Evaluation of insulin sensitivity

The insulin sensitivity was estimated by Intraperitoneal Insulin Tolerance Test (IPITT), oral glucose tolerance test (OGTT) in vivo and the homeostasis model assessment of insulin resistance (HOMA-IR) index. Mice were fasted for 6 h for OGTT and 4 h for IPITT, respectively. Glucose load (2 g/kg bodyweight) was given by oral gavage, and insulin (0.5 IU/kg bodyweight) was administered intraperitoneally. Blood samples were collected from tail vein at 30, 60, 90 and 120 min for OGTT and IPITT and glucose concentration determined using a glucometer (Accu-Check Active; Roche Applied Science, Indianapolis, IN, USA). The area under the glucose-time curve (AUC) was then calculated. HOMA-IR index was calculated from fasting serum insulin and plasma glucose levels using the equation for HOMA=fasting serum insulin (μU/mL)×fasting plasma glucose (mM)/22.5 [10].

2.3. Liver analyses

Total lipids were extracted with chloroform: methanol mixture and liver triglycerides (TG) were measured using standard kits (Stanbio). Liver malondialdehyde (MDA) levels were determined using the method proposed by Ohkawa and expressed as nanomoles per gram of tissue [11,12].

2.4. Histopathological analyses

Tissue samples excised from the liver were fixed with 10% buffered formalin before processing for histology by conventional methods. Five-micrometer step sections of the liver were obtained and stained with hematoxylin and eosin (HE) and oil red O. Masson's Trichrome Stain was used for examination of connective tissue and determination of fibrosis. Stained sections were evaluated (light microscopy at 10× and 40×) by a pathologist (Department of Pathology, University of Texas Southwestern Medical Center, Dallas, TX, USA) in a blinded analysis. Macrovesicular steatosis, hepatocellular ballooning, lobular inflammation (including polymorphonuclear leukocytes) and perisinusoidal fibrosis (Zone 3) were determined histopathologically and graded using the modified classification proposed by Brunt et al [13]. *Macrovesicular steatosis* was graded 0–3 based on the percentage of steatotic hepatocytes: 0 is absent, 1 is less than 33% of the parenchyma, 2 is 33–66% and 3 is more than 66% of the parenchyma. *Hepatocellular ballooning* was evaluated for zonal dislocation and graded in a similar fashion. *Lobular (intra-acinar) inflammation* was graded 0–3 based on inflammatory foci per 20× with a 20× ocular: 0 is absent, 1 is 1–2/20×, 2 is up to 4/20× and 3 is >4/20×. Fibrosis was scored 0–3 based on percentage of zone 3 (perisinusoidal) involved. In addition, other common diagnostic features of NASH including mallory body and glycogenated nuclei were evaluated as either present or absent.

2.5. Protein expressions by Western blot

For Western blot, about 200 mg of liver samples were homogenized in 1 mL of lysis buffer (20 mM Tris, 145 mM NaCl, 10% glycerol, 5 mM EDTA, 1% Triton-X, 0.5% Nonidet P-40, 100 M phenylmethylsulfonyl fluoride, 50 M NaF, 1 mM sodium orthovanadate). Lysates were centrifuged at 8850×g at 4°C for 10 min. The supernatant was collected, and the protein concentration was determined by the Bradford method, using bovine serum albumin as a standard. Samples (1.5 g/mm gel thickness) were heated for 5 min under reducing conditions and loaded on sodium dodecyl sulfate-polyacrylamide gel. Proteins from the gel were then transferred onto nitrocellulose membranes. Electroblots were blocked in Tris buffer NaCl-Tween (TBST) containing 5% skim milk powder at room temperature following which Western blot analysis with specific antibodies (for collagen I, III and IV, PDGF A and B) was carried out. Blots were incubated with antibodies of interest (in TBST buffer and 5% bovine serum albumin) and rocked overnight at 4°C. After a TBST washing procedure, the blots were incubated with horseradish peroxidase–labeled antirabbit antibody (Cell Signaling, Beverly, MA, USA) in skim milk for 1 h at room temperature. The immune reaction was detected by enhanced chemiluminescence. Bands were quantified by scanning densitometry and expressed as arbitrary units.

2.6. RNA isolation and quantification of gene expression by real-time polymerase chain reaction (PCR)

Total RNA from liver tissues was extracted using TRIZOL reagent (Invitrogen, Carlsbad, CA, USA) according to protocols provided by manufacturer. RNA purity was established by agarose gel electrophoresis, and the amount of RNA was quantified by measurement of $A_{260/280}$ ratio. Extracted RNA was reverse-transcribed in 20 μl of reaction mixture containing Superscript III reverse transcriptase (200 U/μl), RNAse inhibitor RNAseOUT (40 U/μl), 25mM $MgCl_2$, RT buffer (50mM KCl, 10mM Tris-HCl- pH 8.3), 50 μM oligo$(dT)_{20}$ primer, 0.1M DTT and 10 mM dNTPs. The reaction mixture was heated to 50°C for 50 min and then terminated at 85°C for 5 min. cDNA (after 1:25 dilution with 0.25 g/L of bovine serum albumin) was amplified with iQ5 Optical System Software, Version 2.0 using platinum Taq DNA polymerase in 25 μl of reaction mixture containing 0.25mM dNTPs, 20.5 μl of SYBR^R Green I qPCR mix (modified hot start DNA polymerase), optimized PCR buffers and appropriate forward and reverse PCR primers. PCR reactions following the first denaturation at 95°C for 15 min (hot start) were carried out using the cycling conditions listed below: 30 cycles (60°C or in accordance to primer melting points less 4–5°C for 45 s, 72°C for 2.5 min for primer extension and 94°C for 30 s for dsDNA denaturation). beta-Actin was amplified in parallel for use as control during normalization. The correct size of PCR products was confirmed by matching the dsDNA size to DNA standard on 2% agarose gel stained with ethidium bromide during electrophoresis. Purity was determined by melting point analysis.

2.7. Statistical analyses

All data are expressed as means±S.E. Differences obtained by unpaired Student's t test were considered significant at P<.05, using SPSS version 15.0 for Windows.

3. Results

The HFD increased body weight (Fig. 1A) and adiposity in C57BL/6J mice (Table 1). No significant difference was observed in the mean food intake (g) of HF groups and control groups over the 20-week period. However, the mean caloric intake of the HF group was significantly greater than control groups (P<.05), and this was attributable to the higher energy content of the HFD. Liver weight (wet) of the HF group was about twofold greater than those of control mice (Table 1). Ratios of liver weights to final body weights in the HF group (0.123±0.011) were approximately 27% higher than low-fat counterparts (0.097±0.008).

Elevated blood glucose, insulin, free fatty acids, leptin, and triglycerides are blood biomarkers associated with liver dysfunction in human NASH. Fasting blood glucose levels of mice fed HFD in our study were significantly higher than controls (Table 2). Mean fasting insulin levels and insulin resistance index determined by the HOMA parameter were also significantly higher in mice fed the HFD, indicating a decline in insulin sensitivity. Compared to controls, mice fed HFD showed impaired response to exogenous insulin challenge in the IPITT as evidenced by the insignificant drop in blood glucose even at the end of 120 min after insulin administration (Fig. 1B). On the other hand, blood glucose level in the control group was observed to begin dropping down beginning 30 min after insulin administration until 120 min when normal levels were achieved. Additionally, a 48% increase in the AUC was seen in mice fed HFD. In the OGTT, plasma

glucose levels peaked 30 min after the oral glucose challenge in both control and HFD groups (Fig. 1C). However, the AUC of the plasma glucose response in mice fed the HFD (calculated as difference from basal levels in each animal) was significantly higher (~98%) than controls ($P<.05$), suggesting pronounced glucose intolerance. Glucose elimination followed first order kinetics thereafter until 120 min following oral gavage.

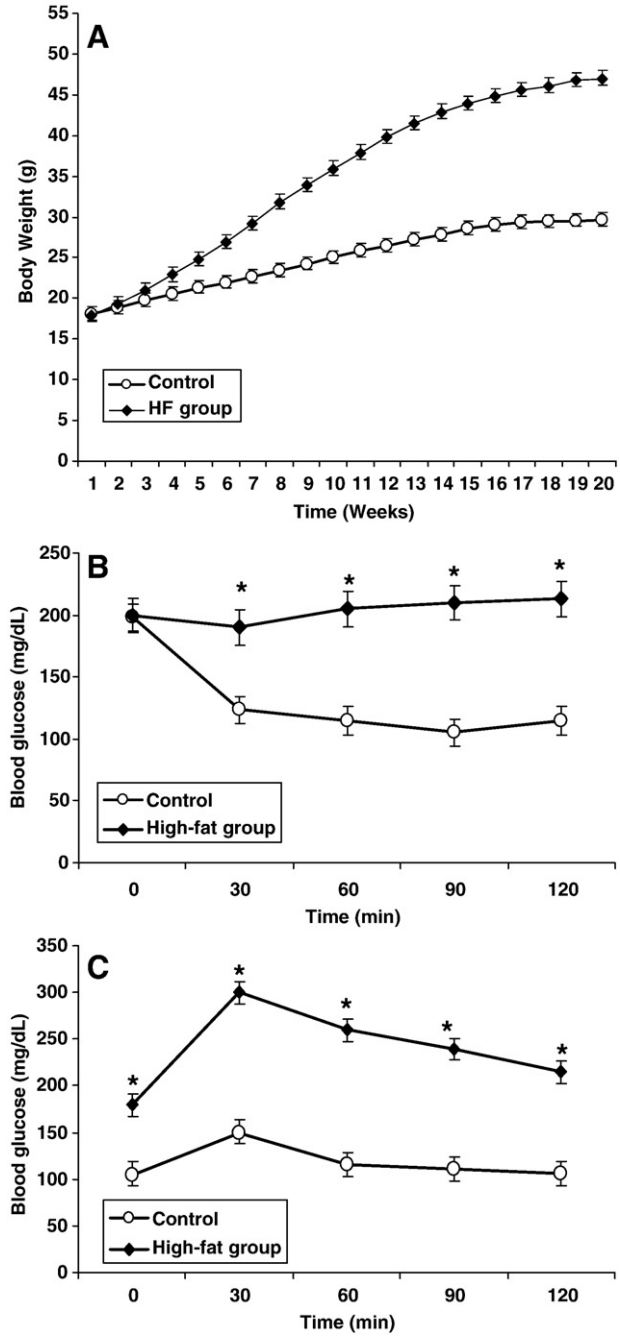

Fig. 1. Adiposity and insulin resistance induced by HFD in C57BL/6J mice. (A) Body weight gain in C57BL/6J mice fed the control or HFD for 20 weeks. (B) Intraperitoneal insulin tolerance test (IPITT) for groups fed control ($n=10$) or HFD ($n=10$): Blood glucose concentration during IPITT at 0, 30, 60, 90, and 120 min after insulin administration (0.5 units/kg body weight). Time 0 represents time when insulin was administered. (C) Oral Glucose Tolerance Test (OGTT) curve for groups fed control ($n=10$) or HFD ($n=10$): Blood glucose concentration at 0, 30, 60, 90, and 120 min after OGTT (2g/kg body weight). Time 0 represents time when glucose was administered. Values are Mean±standard error. $P<.05$.

Table 1
Body weight, food intake and tissue weights of male C57BL/6J mice fed control or HFD for 20 weeks

	Control ($n=20$)	HF group ($n=20$)
Initial body weight, g (5 weeks old)	18.03±1.80[a]	18.00±1.12[a]
Final body weight, g (after 20 weeks)	29.60±2.30[a]	47.03±2.80[b]
Weight gain, g	11.58±2.12[a]	29.03±1.89[b]
Mean Food intake, g/day *	103.25±3.40[a]	108.68±4.50[a]
Mean calorie intake, kcal/day **	339.90±5.10[a]	489.06±4.90[b]
Epididymal fat, g/100 g bodyweight	1.05±0.34[a]	2.02±0.45[b]
Retroperitoneal fat, g/100 g bodyweight	0.60±0.12[a]	1.04±0.16[a]
Omental fat, g/100 g bodyweight	1.02±0.23[a]	2.50±0.31[b]
Liver, g	2.88±0.26[a]	5.79±0.30[b]

[a,b] Data are means±SE of n animals in each group. Means with different letter superscripts across a row are statistically significant, $P<.05$.

* Mean food intake of 20 mice per day in each group.

** Mean calorie intake of 20 mice per day in each group (Calorie density of low-fat diet=3.29 kcal/g diet; HFD=4.50 kcal/g diet).

In addition, hypoadiponectinemia and hyperleptinemia were observed in the HF group, compared to low-fat controls (Table 2). The HFD increased plasma free fatty acids to an average of 40 mg/L greater than control, though not significant ($P=.065$). Plasma triglyceride concentrations were not significantly altered; however, clear hypercholesterolemia was observed in the HF group, due mostly to an increase in low-density lipoprotein cholesterol (LDL-c), associated with no significant alterations in high-density lipoprotein cholesterol (HDL-c) (Table 2).

Status of inflammatory cytokines and biomarkers of oxidative stress were evaluated in both groups. Circulating tumor necrosis factor (TNF)-α and transforming growth factor (TGF)-β 1 levels in the HF group were significantly higher than the control group ($P<.05$). A two-fold increase in plasma resistin levels was induced by HF feeding in the HF group as compared with the control mice ($P<.05$). Compared to the control group, high-sensitivity C-reactive protein (hs-CRP) levels increased by more than 200% ($P<.05$) in the HF group. In addition, elevated plasma MDA levels in the HF group (Table 2) are indicative of oxidative damage associated with fat accumulation and insulin resistance, typically seen in patients with NASH.

A significant ($P<.05$) increase in plasma levels of alanine transaminase (ALT), aspartate transaminase (AST), and alkaline phosphatase (AP) was observed in the HF-fed mice as compared to controls. The average increase in the activity of three enzymes was about 110%, 177% and 170% for ALT, AST and AP, respectively (Fig. 2A). Triglyceride accumulation in livers of HF group (8.9 μmol/100 mg liver tissue) increased by more than 230% compared to controls (2.6 μmol/100 mg liver tissue). Liver tissue MDA that are indicative of oxidative damage with fatty infiltration and cirrhosis was also significantly elevated in

Table 2
Blood biomarkers in male C57BL/6J mice fed control or HFDs for 20 weeks

	Control ($n=20$)	HF group ($n=20$)
Plasma glucose (mg/dl)	109.60±10.80[a]	185.60±13.12[b]
Serum Insulin (μU/mL)	8.51±1.11[a]	12.70±2.03[b]
HOMA	2.30±0.12[a]	5.80±0.89[b]
Serum adiponectin (μg/mL)	6.20±1.40[a]	3.40±0.70[b]
Plasma free fatty acids (mg/L)	251.16±30.10[a]	294.04±34.90[a]
Serum TNF-α (pg/mL)	187.70±10.34[a]	285.30±13.45[b]
Plasma MDA (nmol/mL)	0.65±0.32[a]	1.98±0.41[b]
Plasma leptin (ng/mL)	15.78±2.98[a]	49.87±8.85[b]
Plasma TG (mg/dL)	102.40±9.68[a]	107.60±10.89[a]
Plasma total cholesterol (mg/dL)	87.50±11.34[a]	133.96±12.42[b]
Plasma LDL-c (mg/dL)	34.67±7.89[a]	61.45±13.81[b]
Plasma HDL-c (mg/dL)	24.67±6.88[a]	22.77±7.02[a]
hs-CRP (μg/mL)	18.76±5.67[a]	57.98±9.67[b]
Serum resistin (ng/mL)	17.45±4.67[a]	38.59±9.75[b]
Serum TGF-β (pg/mL)	112.66±31.98[a]	154.09±38.25[b]

[a,b] Data are means±SE of n animals in each group. Means with different letter superscripts across a row are statistically significant, $P<.05$.

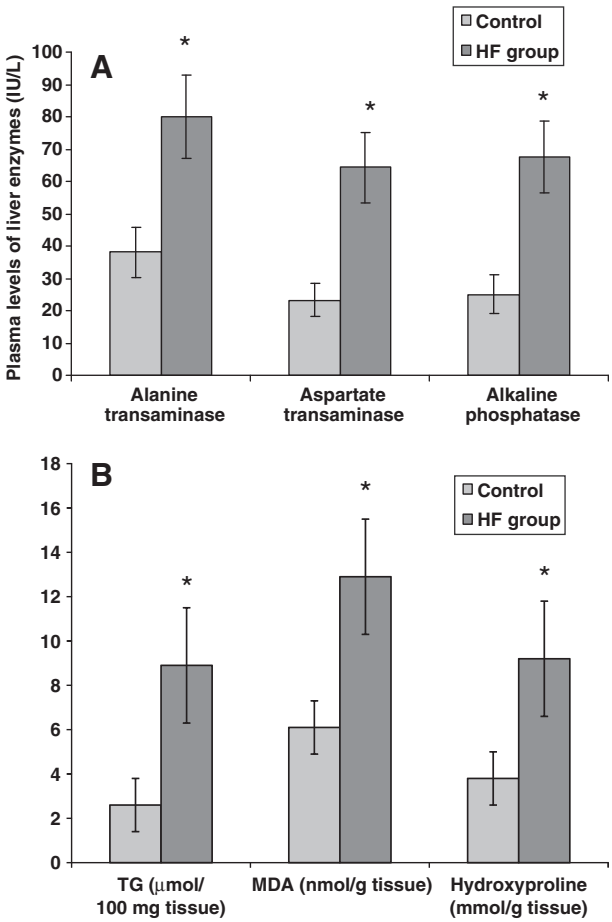

Fig. 2. Plasma levels of ALT, AST and AP (A) and liver triglycerides and MDA (B) in C57BL/6J mice fed control or HFD for 20 weeks (n=20) Values are mean±S.E. *P<.05.

the HF group (9.8 nmol/g tissue) compared to control mice (5.5 nmol/g tissue) after 20 weeks of feeding (Fig. 2B).

3.1. Histological analysis of the liver

Liver histology of the control and HF group was evaluated to investigate the occurrence of NASH. Fig. 3 shows representative images of liver HE-stained sections from both control and animals fed HFD. Fig. 3A–D shows sections of liver from control animals with no steatosis, inflammation or fibrosis. Macrovesicular steatosis was observed in the HF group (Fig. 3E); oil red O staining shows accumulation of triglyceride molecules in the same (Fig. 3F). Fibrosis was observed in the HF group as evidenced by collagen deposition in Masson's Trichrome section (Fig. 3G). In control animals, inflammatory cells were rarely present in the portal tract (Fig. 3D) or in the hepatic parenchyma. The HF group showed increased number of inflammatory cells in the portal tract (Fig. 3H), with lobular inflammation and occasional clusters of neutrophils. To quantify the degree of hepatic inflammation, hepatic neutrophils were counted in HE-stained sections obtained from HF animals (Fig. 4). Neutrophil infiltration in the control animals was insignificant (20±2.56 neutrophils/mm^2); however HFD significantly augmented the number of hepatic neutrophils present within the liver tissue. A 40-fold increase was observed for the HF group (802±98.78 neutrophils/mm^2). Histopathological findings in Fig. 3 are summarized in Table 3. Mallory body and glycogenated nuclei were found to be present in the HF group only.

3.2. Hepatic chemokine and protein expression

Increased collagen (Collagen I, III and IV) expressions (protein and mRNA) observed in the HF group compared to controls confirm development of fibrosis (Fig. 5). A seven- to eightfold increase was found in the protein expressions of collagen I and III in the HF group, while a fivefold increase was observed in collagen IV (Fig. 5A and B). mRNA levels were in concordance with protein expressions (Fig. 5C).

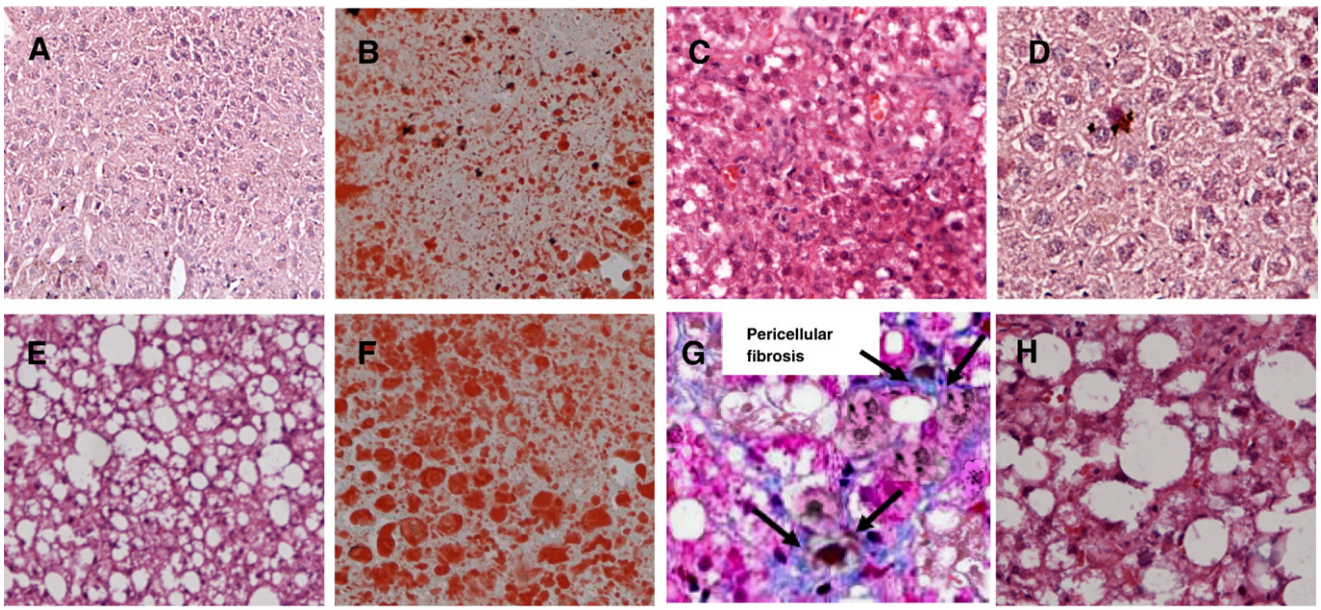

Fig. 3. Histopathological findings in the control and HF groups. (1) Macrovesicular and microvesicular steatosis: (A) control group: normal liver histology (HE ×10) and (E) HF group: macro-vesicular and microvesicular steatosis (HE ×10). (B) Control group: normal liver histology (oil red O ×10) and (F) HF group: triglyceride molecules in cytoplasm during macro-vesicular and micro-vesicular steatosis (oil red O ×10). (2) Pericellular fibrosis: (C) control group: normal liver histology (×20) and (G) HF group: pericellular fibrosis (arrows) (Masson's trichrome ×20). (3) Hepatocyte ballooning and inflammatory cells: (D) control group (HE ×20), and (H) HF group (HE ×20).

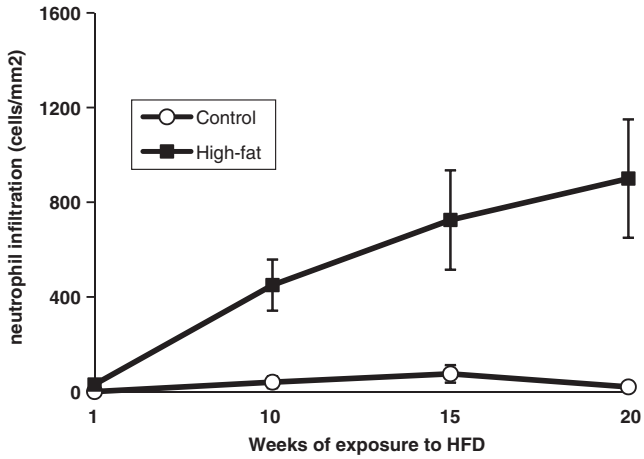

Fig. 4. Neutrophil infiltration in hepatocytes. Hepatic neutrophils were counted in HE-stained sections obtained from control and HF fed animals. Values are expressed as mean±S.E. $P<.05$.

Expressions of PDGF, the predominant mitogen for activated hepatic stellate cells in fibrosis, also followed very similar trends (Fig. 5A–C). These results provide convincing evidence for development of fibrosis, inflammation and extensive hepatic injury characteristic of NASH in animals fed the HF group.

4. Discussion

Increased incidences of NASH and NAFLD worldwide have assumed clinical significance, and establishment of a suitable animal model is highly warranted to facilitate further research and investigations in this area. Earlier studies have shown that C57BL/6J mice develop diet-induced obesity, insulin resistance and MetS; however, the susceptibility of these animals to develop NASH following exposure to HFD has not been thoroughly investigated, except for only one very recent report [9] that presents related data using HFD with lower methionine and choline levels. Methionine and choline are essential for hepatic beta oxidation and very low-density lipoprotein production. Rodents fed the traditional MCD lose significant amounts of weight [6,7,14–16] accompanied by decrease in liver weight (not seen in human NASH). Use of adequate levels of methionine and choline in the HFD in our study led to consistent increase in body weights of mice in the HF group typical of NASH in humans. This leads to the understanding that deficiency of methionine and choline are probably not indispensable for inducing classical symptoms of NASH. Moreover, patients with NASH are rarely exposed to diets deficient in methionine or choline.

At the end of feeding, the body weights of the HF group were significantly higher than the control group and no weight loss (typical of that seen in the human disorder) was observed in the HF group during the entire feeding period.

The constellations of lesions that characterize nonalcoholic steatohepatitis in humans include steatosis, ballooning, lobular inflammation, Mallory's hyaline and perisinusoidal fibrosis [1,2,17,18]. All of these features were adequately demonstrated by this animal model closely replicating pathogenesis of NASH in humans. Liver fibrosis is associated with major alterations in both the quantity and composition of extracellular matrix (ECM) including collagens (I, III and IV), fibronectin and proteoglycans. Activated hepatic stellate cells (HSCs) migrate and accumulate at the sites of tissue repair, secreting large amounts of ECM. PDGF, mainly produced

Table 3
Histopathological findings in the control and HF groups

Histopathological finding	Control group (n=8)	High-fat group (n=10)
Macrovesicular steatosis n (%)		
Grade 0	8 (100)	0 (0)
Grade 1	–	3 (30)
Grade 2	–	4 (40)
Grade 3	–	3 (30)
Hepatocellular ballooning n (%)		
Grade 0	8 (100)	1 (10)
Grade 1	–	3 (30)
Grade 2	–	4 (40)
Grade 3	–	2 (20)
Lobular inflammation (inflammatory cells per 20×)		
Grade 0	7 (87.5)	0 (0)
Grade 1	1 (12.5)	5 (50)
Grade 2	–	4 (40)
Grade 3	–	1 (10)
Fibrosis n (%)		
Grade 0	8 (100)	0 (00)
Grade 1	–	7 (70)
Grade 2	–	3 (30)
Grade 3	–	0 (0)

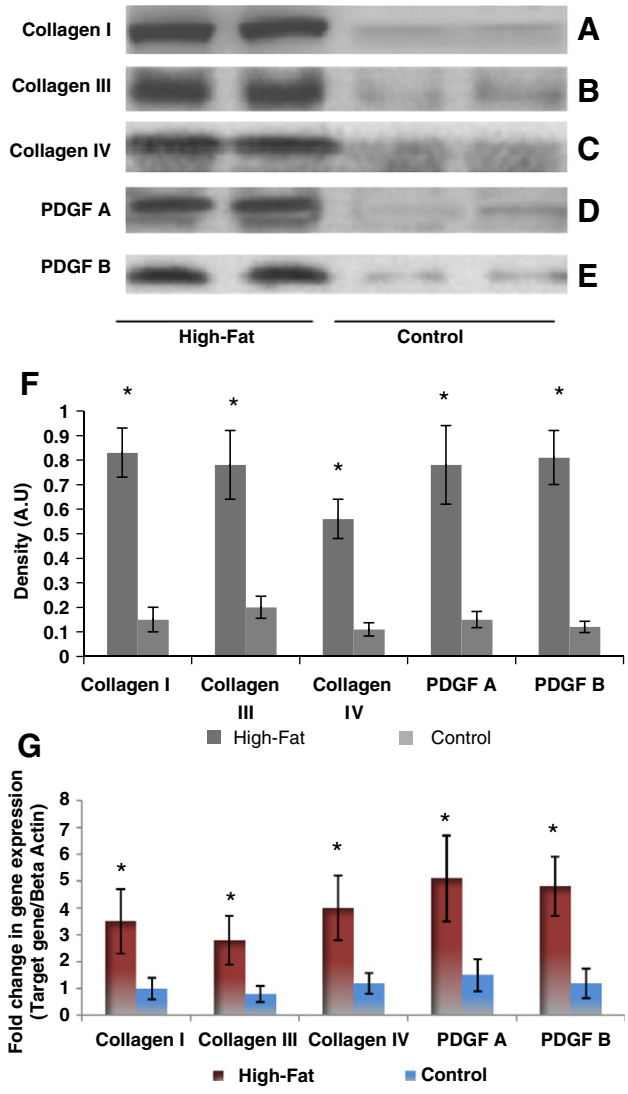

Fig. 5. Effects of HFD on hepatic chemokine and protein expression. (A–E) Hepatic collagen and PDGF expressions. (F) Quantification of protein expression. (G) Hepatic gene expression. The gene expression level was expressed relative to control group ≥1.00) after normalization using the beta-actin gene expression level. Values are expressed as mean±S.E. $P<.05$.

by Kupffer cells, is the predominant mitogen for activated HSCs. Increased collagen mRNA and protein expression associated with increased expressions of predominant PDGFs confirm fibrotic accumulation characteristic of NASH. Neutrophil infiltration that progressively increased with exposure to HFD provides evidence of inflammation. Liver damage accompanied by triglyceride accumulation, elevated plasma levels of diagnostic liver enzymes including ALT, AST and AP and evidence of oxidative damage which are commonly found in patients with NASH [2,17,19] were also found.

Peripheral insulin resistance is one of the most striking features in the pathogenesis of NASH in humans [20,21] but has been inadequately delineated in previous reports [22]. Hyperglycemia, hyperinsulinemia and hypoadiponectinemia were observed in the HF group that also exhibited significantly higher HOMA-IR index compared to the controls. Pronounced glucose intolerance (in OGTT) and impaired response to insulin (in IPITT) adequately delineate peripheral insulin resistance, further corroborated by the huge increase in plasma TNF-α in the HF group accompanied by a corresponding decrease in adiponectin. Patients with NASH have been reported to have elevated TNF-α and low adiponectin levels in plasma [23–25], closely demonstrated by our animal model. The study also recorded significantly higher levels of plasma hs-CRP levels in the HF group (compared to controls). C-reactive protein, a marker of systemic inflammation is an independent clinical feature that distinguishes NASH from simple nonprogressive steatosis. Positive correlation was found between plasma hs-CRP levels and stages of fibrosis in patients with NASH [26].

Leptin, a peptide hormone released by the adipose tissue prevents "lipotoxicity" in liver by limiting triglyceride accumulation. Hyperleptinemia, typically seen in patients with NASH [27], promotes hepatic steatosis due to the failure of leptin to exert its antisteatotic actions inside hepatocytes and/or its pathogenic role in hepatic insulin resistance. In our study, serum leptin levels of HF group were found to be significantly higher than controls. Increased hepatic triglyceride accumulation and high free fatty acid concentrations in plasma of the HF group observed in this study could be partly attributable to diminished leptin entry into cells (in addition to insulin resistance).

Oxidative stress has a well-established role in the development of NASH. Both plasma and liver tissue MDA levels were significantly higher in the HF group than in controls; prolonged exposure of unsaturated lipids in the HFD to free radicals contributes partly to lipid peroxidation in this experimental NASH model. Kupffer cells and stellate cells, involved in the inflammatory sequence in NASH, secrete TGF-β1 as part of the process of fibrosis [28]. Plasma TGF-β1 levels in patients with NASH were significantly higher than NAFLD patients or healthy controls [29]. In our study, significant levels of fibrosis (perisinusoidal) observed in the HF group related well to the significant increase in serum TGF-β1 levels adequately demonstrating the fibrotic effect of the peptide in development of NASH. In addition, liver hydroxyproline levels in the HF group were significantly higher than control group adequately supporting existence of fibrosis.

Long-term HF feeding regimen with adequate levels of methionine and choline has been shown to induce many of the classic histopathological features associated with human NASH in C57BL/6J mice. Damaged liver function, impaired insulin sensitivity, evidence of oxidative stress and associated state of inflammation observed in this mouse model appropriately mimic the metabolic state induced by the condition in humans. Use of a dietary regimen, high in fat and adequate in methionine and choline accompanied by sucrose drinking-induced hyperphagia closely replicates the actual worldwide scenario responsible for increasing incidences of NASH.

Acknowledgment

This research was supported by a grant from Research Enhancement Program (2007-2008) at Texas Woman's University. The authors thank Dr. John Shelton, senior pathologist at UT Southwestern Medical Center for technical support and expertise on histopathological analyses.

References

[1] Ludwig J, Viggiano TR, McGill DB, Ott BJ. Nonalcoholic steatohepatitis: Mayo clinic experiences with a hitherto unnamed disease. Mayo Clin 1980;55:434–8.
[2] Brunt EM. Pathology of nonalcoholic steatohepatitis. Hepatol Res 2005;33:68–71.
[3] Deng QG, She H, Cheng JH, French SW, Koop DR, Xiong S, et al. Steatohepatitis induced by intragastric overfeeding in mice. Hepatology 2005;42(4):905–14.
[4] Anstee QM, Goldin RD. Mouse models in non-alcoholic fatty liver disease and steatohepatitis research. Int J Exp Pathol 2006;87(1):1–16.
[5] Diehl AM. Lessons from animal models of NASH. Hepatol Res 2005;33:138–44.
[6] Weltman MD, Farrell GC, Liddle C. Increased hepatocyte CYP2E1 expression in a rat nutritional model of hepatic steatosis with inflammation. Gastroenterology 1996;111:1645–53.
[7] Leclercq IA, Farrell GC, Field JC, Bell DR, Gonzalez FJ, Robertson GR. CYP2E1 and CYP4A as microsomal catalysts of lipid peroxides in murine nonalcoholic steatohepatitis. J Clin Invest 2000;105:1067–75.
[8] Collins S, Martin TL, Surwit RS, Robidoux J. Genetic vulnerability to diet-induced obesity in the C57BL/6J mouse; physiological and molecular characteristics. Physiol Behav 2002;81:243–8.
[9] Cong WN, Tao RY, Tian JY, Liu GT, Ye F. The establishment of a novel non-alcoholic steatohepatitis model accompanied with obesity and insulin resistance. Life Sci 2008;82:983–90.
[10] Matthews DR, Hosker JP, Rudenski AS, Naylor BA, Treacher DF, Turner RC. Homeostasis model assessment: insulin resistance and beta-cell function from fasting plasma glucose and insulin concentrations in man. Diabetologia 1985;28:412–9.
[11] Esterbauer H, Schaur RJ, Zollner H. Chemistry and biochemistry of 4-hydroxynonenal, malonaldehyde and related aldehydes. Free Radic Biol Med 1991;11:81–128.
[12] Ohkawa H, Ohishi N, Yagi K. Assay for lipid peroxides in animal tissues by thiobarbituric acid reaction. Anal Biochem 1979;95:351–8.
[13] Brunt EM, Janney CG, Di Bisceglie AM, Neuschwander-Tetri BA, Bacon BR. Nonalcoholic steatohepatitis: a proposal for grading and staging the histological lesions. Am J Gastroenterol 1999;94:2467–74.
[14] George J, Pera N, Phung N, Leclercq I, Yun Hou J, Farrell G. Lipid peroxidation, stellate cell activation and hepatic fibrogenesis in a rat model of chronic steatohepatitis. J Hepatol 2003;39:756–64.
[15] London RM, George J. Pathogenesis of NASH: animal models. Clin Liver Dis 2007;11:55–74.
[16] Jansen PLM. Nonalcoholic steatohepatitis. J Med 2004;62:217–24.
[17] Powell EE, Cooksley WGE, Hanson R, Searle J, Halliday JW, Powell LW. The natural history of nonalcoholic steatohepatitis: a follow-up study of forty-two patients for up to 21 years. Hepatology 1990;11:74–80.
[18] Sanyal AJ, Campbell SC, Mirshahi F, Rizzo WB, Contos MJ, Sterling RK, et al. Nonalcoholic steatohepatitis: association of insulin resistance and mitochondrial abnormalities. Gastroenterology 2001;120:1183–92.
[19] Chitturi S, Abeygunasekhara S, Farrell GC, Holmes-Walker J, Hui JM, Fung C, et al. Insulin hypersecretion and specific association with the insulin resistance syndrome. Hepatology 2002;35:373–9.
[20] Marceau P, Biron S, Hould FS, Marceau S, Simard S, Thung SN, et al. Liver pathology and the metabolic syndrome X in severe obesity. J Clin Endocrinol Metab 1999;84:1513–7.
[21] Marchesini G, Brizi M, Morselli-Labate AM, Bianchi G, Bugianesi E, McCullough AJ, et al. Association of non-alcoholic fatty liver disease with insulin resistance. Am J Med 1999;107:450–5.
[22] Rinella ME, Green RM. The methionine-choline deficient dietary model of steatohepatitis does not exhibit insulin resistance. J Hepatol 2004;40:47–51.
[23] Hui JM, Hodge A, Farrell GC, Kench JG, Kriketos A, George J. Beyond insulin resistance in NASH:TNF-alpha or adiponectin? Hepatology 2004;40:46–54.
[24] Kaser S, Moschen A, Cayon A, Kaser A, Crespo J, Pons-Romero F, et al. Adiponectin and its receptors in non-alcoholic steatohepatitis. Gut 2005;54:117–21.
[25] Tilg H, Diehl AM. Cytokines in alcoholic and nonalcoholic steatohepatitis. N Engl J Med 2000;343:1467–76.
[26] Yoneda M, Mawatari H, Fujita K, Iida H, Yonemitsu K, Kato S, et al. High-sensitivity C-reactive protein is an independent clinical feature of nonalcoholic steatohepatitis (NASH) and also of the severity of fibrosis in NASH. J Gastroenterol 2007;42(7):573–82.
[27] Uygun A, Kadayifci A, Yesilova Z, Erdil A, Yaman H, Saka M, et al. Serum leptin levels in patients with nonalcoholic steatohepatitis. Am J Gastroenterol 2000;95(12):3584–9.
[28] Oberhammer FA, Pavelka M, Sharma S, Tiefenbacher R, Purchio AF, Bursch W, Schulte-Hermann R. Induction of apoptosis in cultured hepatocytes and in regressing liver by transforming growth factor-β1. Proc Natl Acad Sci USA 1992;9:5408–12.
[29] Hasegawa T, Yoneda M, Nakamura K, Makino I, Terano A. Plasma transforming growth factor-b1 level and efficacy of α-tocopherol in patients with non-alcoholic steatohepatitis: a pilot study. Aliment Pharmacol Ther 2001;15:1667–72.